DOI: 10.25092/baunfbed.340575 *J. BAUN Inst. Sci. Technol., 19(2), 123-136, (2017)*

The effect of molecular interference on coherent scattering

Aysun BÖKE*

Balıkesir University, Faculty of Arts and Sciences, Department of Physics

Geliş Tarihi (Recived Date): 04.07.2017
Kabul Tarihi (Accepted Date): 09.08.2017

Abstract

The effect of molecular interference on coherent scattering is studied for human tissues (liver, kidney, muscle and fat). The coherent scattering cross sections are computed by numerical integration. The calculation of molecular form factors is performed as function of the momentum transfer variable formulated with $x=\sin(\theta/2)/\lambda$ in the presence of small concentrations of different elements constituting tissue. It is seen that theoretical values of molecular form factors can be used in the region ($x \geq 1$ Å^{-1}) where there is no experimental data. Because of the lack of data on calculation of coherent scattering of tissues, the results of this study will provide valuable knowledge in literature.

***Keywords**: Coherent (Rayleigh) scattering, interference effect, tissue.*

Koherent saçılma üzerine moleküler girişimin etkisi

Özet

Koherent saçılma üzerine moleküler girişimin etkisi, insan dokuları (karaciğer, böbrek, kas ve yağ) için çalışılmıştır. Koherent saçılma tesir kesitleri nümerik integrasyonla hesaplanmıştır. Moleküler form faktörlerin hesabı, $x=\sin(\theta/2)/\lambda$ ile formüle edilen momentum transfer değişkeninin bir fonksiyonu olarak, dokuyu oluşturan farklı elementlerin küçük konsantrasyonlarının varlığında gerçekleştirilmiştir. Moleküler form faktörlerin teorik değerlerinin, deneysel verilerin olmadığı bölgede ($x \geq 1$ Å^{-1}) kullanılabileceği görülmüştür. Dokuların koherent saçılmasının hesabı üzerine verilerin eksikliğinden dolayı, bu çalışmanın sonuçları literatürde değerli bilgi temin edecektir.

***Anahtar kelimeler**: Koherent (Rayleigh) saçılma, girişim etkisi, doku.*

* Aysun BÖKE**,** aysun@balikesir.edu.tr, http://orcid.org/0000-0002-0108-6825

1. Introduction

Coherent scattering which gives rise to interference effects is found to be the most significant scattering mechanism. These interference effects are most important in the forward direction, where the path length differences are small. Interference effects are commonly used in low-energy x-ray diffractometry for material characterization to get information about the atomic and molecular structure. It is concluded by Leliveld et al [1] that Monte Carlo calculations are significantly in error when interference effects are ignored in the model for coherent scattering. The predominance of coherent scattering in photon transport occurrences at low x allows the exploitation of its dependence on molecular interference effects which results in the diffraction pattern itself in terms of tissue characterization. However, practically every molecular compound has its own diffraction pattern, which is not easy to compute or measure. It is, therefore, advisable that the usual tabulations of coherent scattering data performed in the frame of the independent atomic modeling (IAM) are updated or replaced with an appropriate customization [2].

Reliable photon cross section data are required in several fields that include analytical techniques (X-ray fluorescence, electron probe microanalysis, particle included x-ray emission), medical applications (radiology, radiotherapy, nuclear medicine), detector design and quantification, shielding design and industrial quality control [3]. A new method for the determination of molecular scattering differential cross sections for compounds has been early worked [4, 5]. The renewed interest in radiological diagnosis based on x-ray coherent scattering demands careful modeling of the proposed techniques to be optimized for clinical practice [6-8]. A library of the scattering properties of tissues will be an important tool for the developing field of x-ray scatter imaging [8]. Coherent scattering cross sections and molecular form factors of tissues are required especially in a low-energy application, such as mammographic imaging**.** Their knowledge would help to understand artifacts due to single and multiple scattering in computerized tomography (CT) scanners.

The interference effects are well known in crystallography. A collimated beam of x-rays incident on a crystal produce a scattered beam, very intense in certain directions, corresponding to constructive interference from waves reflected from layers of atoms in the crystal. Interference is possible because the wavelength of the x-rays is about the atomic spacing in a solid ($\approx$1 $Å^{-1}$). In an amorphous solid, the arrangement of the molecules is not completely featureless. There is still a weak ordering. Therefore, interference is also possible for coherent x-ray scattering from amorphous materials. In contrast to the sharp diffraction patterns of crystals, amorphous materials generate only one or more broad halos [1].

Some researchers exerted an effort to provide molecular form factors including molecular interference effects from experimental data. Morin [9] have tabulated molecular form factor for liquid water. Tartari et al [2] developed molecular form factor tabulations for coherent scattering of photons in tissues. Peplow and Verghese [10] extracted molecular form factors from experimental measurements. Recently, King et al [11] have reported the experimental molecular form factors of tissues. Rao et al [12] have calculated x-ray scattering cross sections for molecules, plastics, tissues, and few biological materials. Hubbell [13] has tabulated the cross sections for elements and compounds which include muscle and compact bone tissue.

As far as it is known by now, there has not been any theoretical prediction on the molecular form factors obtained by using the relativistic modified atomic form factor (RMFF) approximation. The results are presented in Table 1 for use by others modeling photon transport problems. The calculation of molecular form factors is made according to tissue compositions, taken from ICRP 23 [14] for kidney, muscle, fat and from Kosanetzky et al [15] for liver. The number of elements involved in tissue compositions is 5 for liver, 47 for kidney, 44 for muscle and 3 for fat. The molecular coherent scattering cross sections are computed both with inclusion and without inclusion of the molecular interference effects. The new data are listed in Table 2 for this time by this study. Comparison on coherent cross section is presented in Table 3 for muscle tissue.

2. Theoretical background

2.1. The molecular form factors

Mainly there are two approaches, to obtain a detailed description of coherent scattering process: the numerical partial wave calculations of elastic scattering amplitudes using second-order S-matrix-theory and the form factor (FF) approximation. The FF approximation is often used to predict the Rayleigh scattering amplitudes. A detailed explanation on the FF approximations is given by Böke [16].

Theoretical predictions of the FF are based on nonrelativistic and relativistic individual electron and total atom wave functions. There is also the RMFF approximation, which accounts for the correction for binding of the atomic electrons. Hubbell et al [17], Hubbell and Øverbø [18] and Schaupp et al [19] have tabulated the nonrelativistic, relativistic and relativistic modified FF for a wide range of momentum transfer and for all elements, respectively. Detailed tabulation of the atomic FF is also presented by Chantler [20].

Clearly, experimental FF results are in better agreement with the RMFF approximation. The findings suggesting the superiority of the RMFF theory have been reported earlier [16, 19, 21-35]. It has been established both from comparison of theoretical results and from experiments that the RMFF, in general, produces better results than other choices of the FF [34].

The FF is usually calculated assuming a free atom with a spherically symmetric electron charge distribution. Furthermore, when the FF of a mixture of elements is calculated, it is assumed that the FF combines independently. As a result of these assumptions the scattering cross section model for coherent scattering only accounts for the interference between scatterings from electrons in the same atom.

When considering a molecule, the FF is often calculated [36] by adding the squares of the individual atomic FF, weighted by their respective atomic abundances n_i.

$$f_{mol}^2(x) = \Sigma_i n_i f^2(x, Z_i) \tag{1}$$

For most composite materials, the atomic abundances are not known so the molecular coherent scatter FF can be expressed [2, 6, 10, 37-39] without knowing the molecular formula by using the free atom model:

$$\frac{f_{mol}^2(x)}{W} = \Sigma_i \frac{w_i}{M_i} f^2(x, Z_i) \quad (2)$$

where w_i, M_i, Z_i and $f(x,Z_i)$ are the mass fraction, the atomic mass, the atomic number and the atomic FF of element i, respectively. W is the molecular weight. The $f_{mol}(x)$, function of the momentum transfer variable x, is the molecular FF.

This approach does not consider the interference effects between the electrons of the various atoms when they are all assembled into the molecule. The approach also leaves out intermolecular interference effects, which depend on the spatial distribution of molecules in the material. Since the sum rule ignores these effects, it is called the free-gas model.

2.2. The coherent scattering cross section

The coherent (Rayleigh) scattering cross section per molecule is given as

$$\sigma_{mol} = \int_{\theta=0}^{\theta=\pi} d\sigma^T(\theta) \left| f_{mol}(x) \right|^2 \quad (3)$$

Total coherent scattering cross section is computed by using numerical integration of the Thomson [40] formula weighted by the $f^2_{mol}(x)$ defined in Eq. (3). The differential Thomson scattering cross section per electron, is given as

$$\frac{d\sigma^T}{d\Omega} = \frac{r_e^2}{2}(1 + \cos^2\theta) \quad (4)$$

where the classical electron radius is $r_e = e^2/m_e c^2$.

3. Results and discussion

The theoretical FF values of tissues are calculated by using formula defined in Eq. (2) from x=0 Å^{-1} to 10^2 Å^{-1} and listed in Table 1. In calculations, the RMFF approximation of Schaupp et al [19] is used. The theoretical FF values are shown in Figures 1-4 together with those of measured by King et al [11] and Peplow and Verghese [10].

The theoretical FF values provide an approximation in the region ($x \geq 1$ Å^{-1}) where there is no experimental data. As discussed by some researchers [9, 10, 13, 38, 41, 42, 43], the measured values approach the IAM values at large values of x. As can be seen in figures 1-4, the theoretical and experimental FF values are very close to each other around x=1 Å^{-1}.

The differences between the experimental and theoretical FF are most important for low x values. These differences are due to intramolecular and intermolecular interferences effects. It is clear from figures 1-4 that the experimental FF values differ with theoretical predictions. The FF values show a strong increase for small x values where interference effects are big. As a result of interference, the angular distribution does not

peak around zero scatter angle but at a specific angle. This peak angle depends on the primary photon energy and the type and structure of the scatter material.

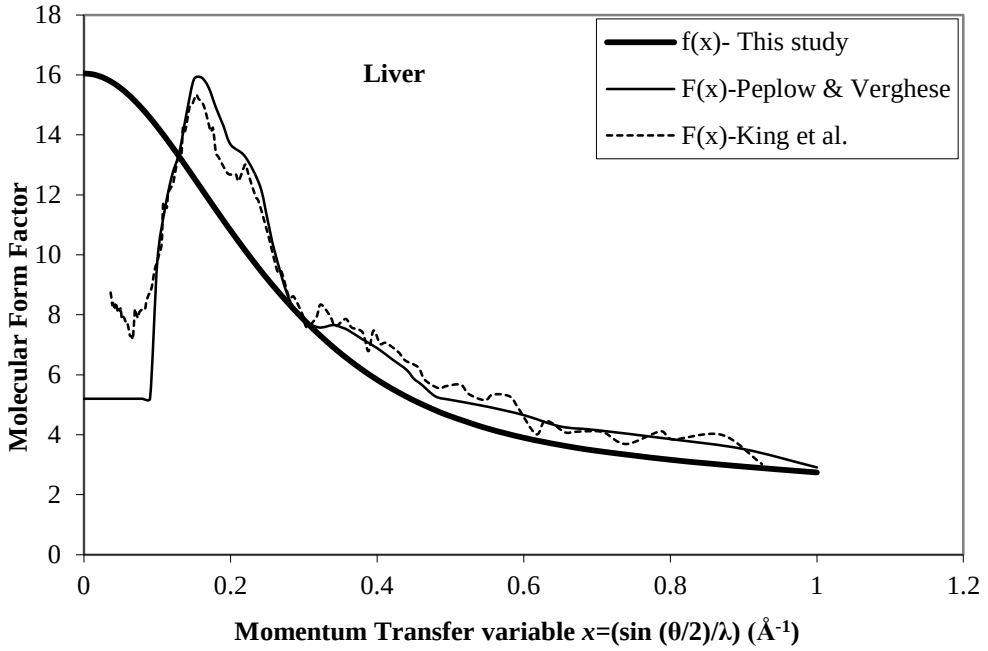

Figure 1. Comparison between experimental and theoretical molecular form factors for liver. The $F(x)$ is experimental data of Peplow and Verghese [10] and King et al [11]. The $f(x)$ is theoretical data calculated in this study with independent atomic modeling (IAM).

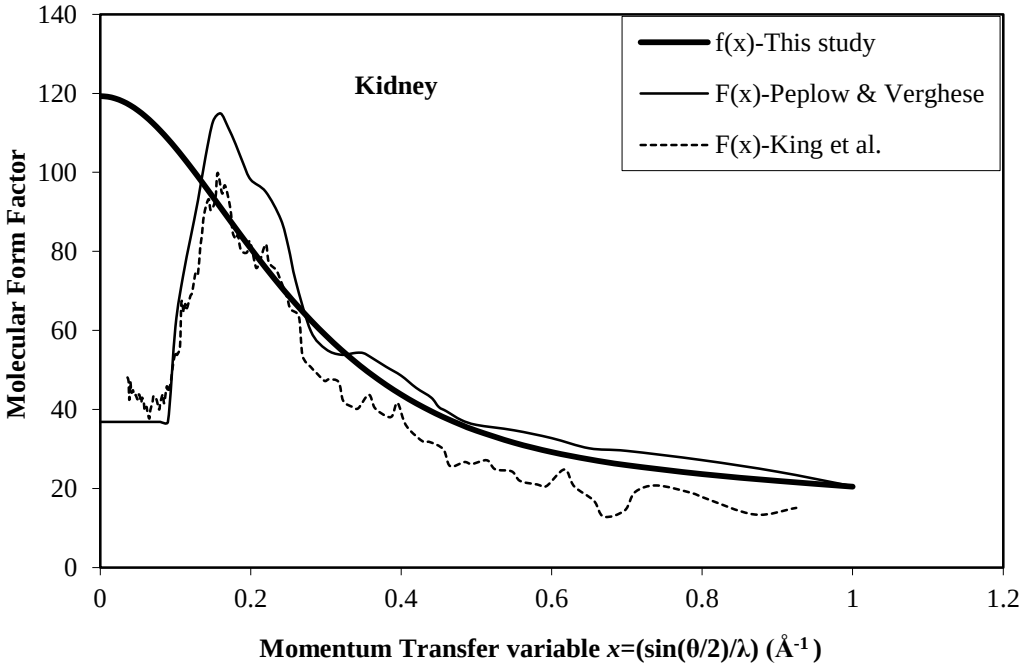

Figure 2. For kidney (see Figure 1 for explanation)

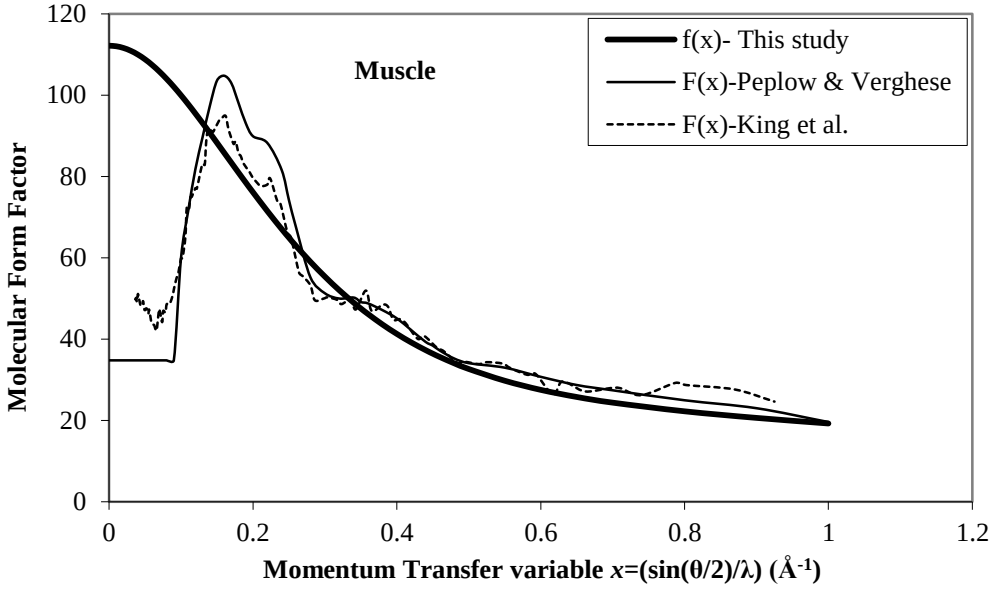

Figure 3. For muscle (see Figure 1 for explanation)

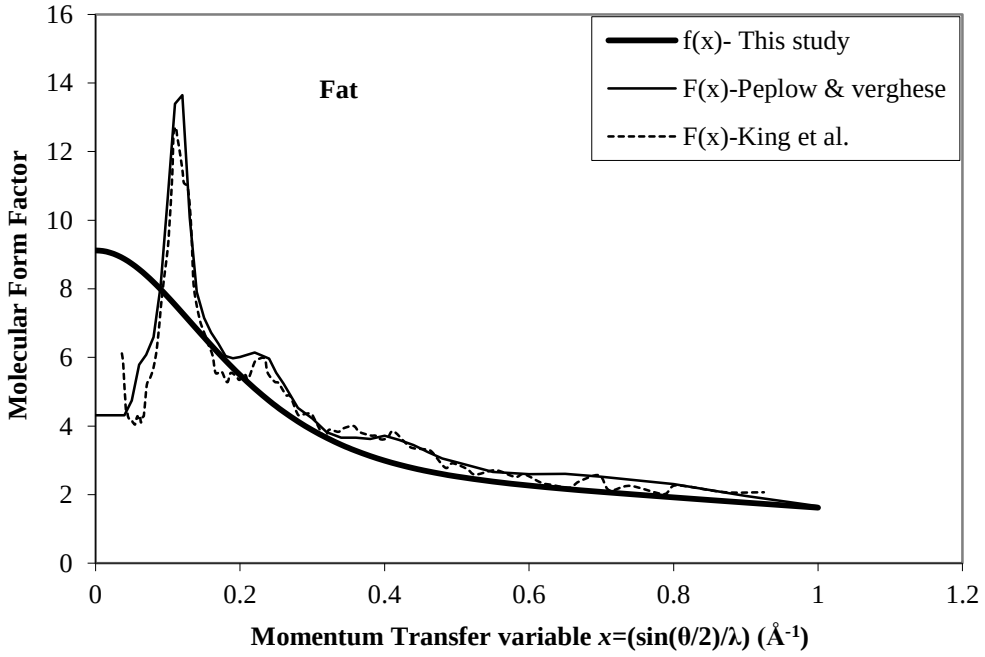

Figure 4. For fat (see Figure 1 for explanation)

The molecular coherent scattering cross sections (σ_{mol}) have been calculated by numerically performing the integration defined in Eq. (3) in the energy range of 1-150 keV. Table 2 shows theoretical results of molecular coherent scattering. The coherent data calculated with inclusion of the molecular interference effects are achieved by using both experimental FF [11] which covers values of $x \leq 0.925$ Å^{-1} and theoretical FF which covers values of $1 \leq x \leq 10^2$ Å^{-1}. Also, the coherent data calculated without inclusion of the molecular interference effects are obtained by using only theoretical FF

which covers values of $0 \leq x \leq 10^2$ Å^{-1}. In Table 3, the molecular coherent coefficients (σ_{mol}) are compared for only muscle tissue because of the lack of data in the literature.

Table 1. The theoretical molecular form factors calculated by using the relativistic modified atomic form factor (RMFF) are presented for liver, kidney muscle and fat tissue.

x (Å^{-1})	$f_{mol}(x)_{\text{Liver}}$	$f_{mol}(x)_{\text{Kidney}}$	$f_{mol}(x)_{\text{Muscle}}$	$f_{mol}(x)_{\text{Fat}}$
0	16.0490	119.2947	112.1872	9.1180
1.00E-02	16.0288	119.1455	112.0484	9.1021
2.00E-02	15.9677	118.6976	111.6308	9.0533
3.00E-02	15.8684	117.9678	110.9507	8.9742
4.00E-02	15.7313	116.9600	110.0114	8.8662
5.00E-02	15.5586	115.6929	108.8305	8.7307
6.00E-02	15.3534	114.1861	107.4261	8.5719
7.00E-02	15.1183	112.4606	105.8167	8.3924
8.00E-02	14.8561	110.5355	104.0202	8.1952
9.00E-02	14.5729	108.4575	102.0808	7.9844
1.00E-01	14.2680	106.2188	99.9900	7.7615
1.10E-01	13.9477	103.8665	97.7921	7.5319
1.20E-01	13.6143	101.4174	95.5026	7.2960
1.30E-01	13.2725	98.9047	93.1524	7.0592
1.40E-01	12.9225	96.3305	90.7432	6.8215
1.50E-01	12.5686	93.7258	88.3042	6.5859
1.60E-01	12.2126	91.1036	85.8476	6.3527
1.70E-01	11.8570	88.4832	83.3908	6.1257
1.80E-01	11.5036	85.8766	80.9462	5.9039
1.90E-01	11.1545	83.2995	78.5277	5.6901
2.00E-01	10.8112	80.7637	76.1471	5.4831
2.20E-01	10.1433	75.8244	71.5065	5.0946
2.40E-01	9.5066	71.1092	67.0731	4.7392
2.50E-01	9.2042	68.8672	64.9640	4.5750
2.60E-01	8.9095	66.6814	62.9067	4.4190
2.80E-01	8.3517	62.5384	59.0055	4.1328
3.00E-01	7.8354	58.6993	55.3882	3.8782
3.20E-01	7.3582	55.1469	52.0394	3.6525
3.40E-01	6.9223	51.8983	48.9759	3.4525
3.50E-01	6.7184	50.3767	47.5399	3.3632
3.60E-01	6.5244	48.9281	46.1728	3.2788
3.80E-01	6.1610	46.2133	43.6101	3.1250
4.00E-01	5.8334	43.7624	41.2957	2.9902
4.20E-01	5.5360	41.5349	39.1911	2.8724
4.40E-01	5.2697	39.5371	37.3030	2.7693
4.50E-01	5.1454	38.6043	36.4210	2.7225
4.60E-01	5.0289	37.7286	35.5929	2.6790
4.80E-01	4.8111	36.0906	34.0434	2.5988
5.00E-01	4.6160	34.6221	32.6537	2.5275
5.50E-01	4.2120	31.5737	29.7674	2.3802
6.00E-01	3.8998	29.2108	27.5280	2.2643

Table 1. (Continued.)

x (Å^{-1})	$f_{mol}(x)_{\text{Liver}}$	$f_{mol}(x)_{\text{Kidney}}$	$f_{mol}(x)_{\text{Muscle}}$	$f_{mol}(x)_{\text{Fat}}$
6.50E-01	3.6565	27.3660	25.7792	2.1659
7.00E-01	3.4620	25.8886	24.3786	2.0789
8.00E-01	3.1654	23.6388	22.2487	1.9193
9.00E-01	2.9379	21.9215	20.6286	1.7669
1.00E+00	2.7424	20.4551	19.2498	1.6189
1.10E+00	2.5635	19.1208	17.9983	1.4763
1.20E+00	2.3906	17.8354	16.7939	1.3398
1.30E+00	2.2243	16.6015	15.6380	1.2118
1.40E+00	2.0647	15.4193	14.5305	1.0933
1.50E+00	1.9110	14.2803	13.4628	0.9848
1.60E+00	1.7646	13.1962	12.4459	0.8860
1.70E+00	1.6263	12.1711	11.4838	0.7968
1.80E+00	1.4965	11.2091	10.5804	0.7164
1.90E+00	1.3755	10.3120	9.7376	0.6443
2.00E+00	1.2632	9.4792	8.9548	0.5799
2.20E+00	1.0638	8.0002	7.5639	0.4709
2.40E+00	8.9571E-01	6.7520	6.3893	0.3841
2.50E+00	8.2215E-01	6.2058	5.8752	0.3475
2.60E+00	7.5502E-01	5.7071	5.4057	0.3149
2.80E+00	6.3772E-01	4.8355	4.5851	0.2594
3.00E+00	5.4018E-01	4.1105	3.9022	0.2150
3.30E+00	4.2392E-01	3.2457	3.0875	0.1640
3.50E+00	3.6217E-01	2.7860	2.6541	0.1378
3.60E+00	3.3537E-01	2.5863	2.4658	0.1266
3.90E+00	2.6782E-01	2.0824	1.9905	9.8932E-02
4.00E+00	2.4878E-01	1.9401	1.8562	9.1321E-02
4.20E+00	2.1571E-01	1.6927	1.6224	7.8165E-02
4.60E+00	1.6379E-01	1.3029	1.2536	5.8000E-02
5.00E+00	1.2625E-01	1.0194	0.9845	4.3784E-02
5.40E+00	9.8635E-02	0.8093	0.7843	3.3565E-02
5.50E+00	9.2922E-02	0.7656	0.7425	3.1481E-02
5.80E+00	7.8043E-02	0.6513	0.6330	2.6102E-02
6.00E+00	6.9710E-02	0.5868	0.5711	2.3123E-02
6.20E+00	6.2453E-02	0.5304	0.5168	2.0550E-02
6.60E+00	5.0518E-02	0.4368	0.4263	1.6375E-02
7.00E+00	4.1262E-02	0.3633	0.3549	1.3188E-02
7.40E+00	3.3989E-02	0.3049	0.2979	1.0724E-02
8.00E+00	2.5792E-02	0.2380	0.2322	7.9932E-03
9.00E+00	1.6867E-02	0.1633	0.1582	5.0923E-03
1.00E+01	1.1438E-02	0.1164	0.1114	3.3784E-03
1.10E+01	7.9953E-03	8.5726E-02	8.0477E-02	2.3180E-03
1.20E+01	5.7319E-03	6.4901E-02	5.9464E-02	1.6355E-03
1.40E+01	3.1360E-03	3.9865E-02	3.4298E-02	8.7227E-04
1.60E+01	1.8311E-03	2.6329E-02	2.0972E-02	4.9941E-04
1.80E+01	1.1235E-03	1.8372E-02	1.3427E-02	3.0162E-04
2.00E+01	7.1662E-04	1.3369E-02	8.9237E-03	1.8977E-04
2.20E+01	4.7111E-04	1.0053E-02	6.1208E-03	1.2319E-04
2.50E+01	2.6183E-04	6.8575E-03	3.6489E-03	6.7218E-05
2.80E+01	1.5073E-04	4.8649E-03	2.2819E-03	3.7884E-05
3.10E+01	8.8335E-05	3.5466E-03	1.4831E-03	2.1620E-05

Table 1. (Continued.)

x (Å^{-1})	$f_{mol}(x)_{\text{Liver}}$	$f_{mol}(x)_{\text{Kidney}}$	$f_{mol}(x)_{\text{Muscle}}$	$f_{mol}(x)_{\text{Fat}}$
3.50E+01	4.3309E-05	2.3968E-03	8.7668E-04	1.0020E-05
4.00E+01	1.6372E-05	1.5198E-03	4.8486E-04	3.1719E-06
4.50E+01	4.6102E-06	9.9039E-04	2.8667E-04	2.3799E-07
5.00E+01	3.4685E-06	6.5998E-04	1.8289E-04	1.3157E-06
6.00E+01	6.4303E-06	3.1065E-04	9.8708E-05	2.1072E-06
7.00E+01	6.5184E-06	1.5940E-04	7.2035E-05	2.0422E-06
8.00E+01	5.7895E-06	9.2446E-05	5.8703E-05	1.7863E-06
9.00E+01	4.9401E-06	6.2516E-05	4.9001E-05	1.5160E-06
1.00E+02	4.1660E-06	4.8090E-05	4.1116E-05	1.2773E-06

In the numerical integration, the integration variable was taken as 1-cosθ, from which the values of x=sin(θ/2)/λ(Å)=[(1-cosθ)/2]$^{1/2}$/λ(Å) could be computed close to θ=0. The integration range used, was from 1-cosθ = 10^{-16} to 2.0 (θ=0.0000008538° to 180°), divided into intervals in the logarithm of 1-cosθ by using a modified formula [16]. However, in the studies of Hubbell et al [17] and Hubbell and Øverbø [18], the integration range was taken from 1-cosθ =10^{-12} to 2.0 (θ=0.000081° to 180°). Since the FF values change quickly for small x values, the integration mesh points can be increased in this range. Thus, with taking into account of the smaller scattering angles, the more accurate data are obtained.

The total coherent cross section is sensitive to the effects of interference at very low energies, where the integration covers values of small x, and it causes a significant decrease in the coherent cross section. It is observed in Table 2 at the photon energies below 3 keV for liver, fat and below 10 keV for kidney, muscle. For E<12 keV, the integration uses only values of x < 1 Å^{-1} and so total coherent coefficients (σ_{mol}) use experimental data. For E>12 keV, the integration extends to value of $x \geq 1$ Å^{-1} and so coherent coefficients (σ_{mol}) use both experimental and theoretical data.

In Table 3, the differences between this study and Hubbell [13] are due to the inclusion of the molecular interference effects and smaller scattering angles. It is expected that the dissimilarity can be greater for values of E<10 keV. Besides, the reason for such a discrepancy can come from differences in the molecular weight and the elemental composition fractions. The number of elements involved in muscle tissue composition is 44 in this study and 10 in the study of Hubbell [13].

Table 2. The total coherent scattering cross-section σ_{mol} (barns/molecule) of tissues.

	σ_{mol}-Liver		σ_{mol}-Kidney		σ_{mol}-Muscle		σ_{mol}-Fat	
E (keV)	with interference effect	without interference effect	with interference effect	without interference effect	with interference effect	without interference effect	with interference effect	without interference effect
1	45.9100	153.2253	1360.7069	8473.7275	1570.2352	7499.0864	19.6342	48.0460
2	90.7593	126.4533	3335.7932	7010.0649	3547.7458	6212.3218	34.3633	37.3825
3	98.9185	98.8653	3412.0435	5494.7847	3617.6020	4875.1875	28.7880	27.8087
4	71.5013	76.6422	2663.6816	4268.1299	2789.2080	3789.6260	20.5948	20.9681
5	64.5838	60.2934	2223.0249	3362.1841	2489.5054	2986.4194	19.7620	16.3585
6	54.1068	48.5360	1733.2545	2708.8255	2037.8326	2406.5234	15.9805	13.2212
7	45.3490	39.9954	1494.8799	2233.2874	1728.4368	1984.1794	13.2715	11.0071
8	39.4252	33.6907	1252.8330	1881.7279	1508.6470	1671.7978	10.3944	9.3915
9	35.0374	28.9004	1151.7255	1614.3142	1379.2832	1434.1092	10.1485	8.1637
10	30.1153	25.1526	883.0848	1404.9582	1194.0696	1248.0005	9.1759	7.1911
11	26.1340	22.2135	795.2767	1240.7405	1107.8997	1102.0291	7.3087	6.4083
12	24.6963	19.7862	672.7060	1105.0798	1008.6858	981.4468	7.1749	5.7512
13	22.1709	17.7739	643.8166	992.6118	929.2661	881.4985	6.6778	5.1929
14	18.7698	16.0876	600.6222	898.3944	773.7952	797.7961	5.8072	4.7132
15	16.6032	14.6652	591.4788	818.9498	691.7674	727.2361	5.0182	4.2994
16	16.2657	13.4032	541.5691	748.4574	671.5236	664.6310	4.3533	3.9307
17	14.9613	12.3112	460.9127	687.4902	621.2481	610.4992	4.3783	3.6073
18	13.9855	11.3496	459.9122	633.8143	590.5635	562.8478	4.0663	3.3203
19	12.2935	10.4960	397.5900	586.1762	526.5774	520.5624	3.7723	3.0643
20	11.3967	9.7272	386.5171	543.2748	477.2865	482.4821	3.4562	2.8335
25	8.3337	6.9077	289.9623	385.9759	354.5598	342.8633	2.4007	1.9908
35	4.7623	3.9472	164.3038	220.7589	204.7286	196.1726	1.3549	1.1256
40	3.6108	3.1257	130.3343	174.8762	156.1602	155.4213	1.0692	0.8894
45	3.0209	2.5404	110.0203	142.1797	132.8127	126.3776	0.7889	0.7213
50	2.5159	2.1021	90.7065	117.6790	109.6588	104.6104	0.7088	0.5960
55	2.0124	1.7684	72.1323	99.0225	89.3632	88.0341	0.5930	0.5005
60	1.6830	1.5104	67.4962	84.5942	74.3823	75.2127	0.4836	0.4267
65	1.5407	1.3022	56.4025	72.9431	67.7525	64.8577	0.4187	0.3674
70	1.3556	1.1346	48.5775	63.5629	59.3014	56.5205	0.3801	0.3196
75	1.1427	0.9971	40.7387	55.8691	52.0226	49.6816	0.3400	0.2806
80	1.0089	0.8827	37.9116	49.4654	44.3419	43.9890	0.2949	0.2481
85	0.8759	0.7889	35.5850	44.2139	39.0009	39.3207	0.2495	0.2214
90	0.8330	0.7074	31.4060	39.6476	37.0810	35.2610	0.2157	0.1983
95	0.7648	0.6381	26.7319	35.7694	33.4251	31.8128	0.2103	0.1788
100	0.6859	0.5782	25.4513	32.4142	30.2543	28.8296	0.1908	0.1618
105	0.6142	0.5263	21.9071	29.5048	27.7133	26.2427	0.1779	0.1472
110	0.5437	0.4814	20.1043	26.9941	24.4119	24.0103	0.1583	0.1345
115	0.5069	0.4417	19.9941	24.7679	22.3494	22.0307	0.1396	0.1234
120	0.4515	0.4075	18.5288	22.8527	20.1457	20.3276	0.1281	0.1137
125	0.4265	0.3763	16.6722	21.1056	19.5911	18.7739	0.1155	0.1049
130	0.4095	0.3486	15.3619	19.5530	18.1684	17.3931	0.1103	9.7206-2
135	0.3862	0.3239	13.6369	18.1669	17.0107	16.1604	0.1063	9.0276-2
140	0.3581	0.3016	13.1138	16.9190	15.7899	15.0506	9.9349-2	8.4032-2
145	0.3353	0.2815	12.1636	15.7897	15.1124	14.0461	9.2856-2	7.8405-2
150	0.3003	0.2635	10.9459	14.7833	13.7666	13.1512	8.8442-2	7.3370-2

Table 3. Comparison of coherent scattering coefficients (m^{-1}) for muscle tissue.

E(keV)	This study	Hubbell [13]
10	21.309	18.408
15	12.345	10.088
20	8.517	6.344
30	4.465	3.224
40	2.787	1.872
50	1.957	1.248
60	1.327	0.936
80	0.791	0.520
100	0.540	0.416
150	0.246	0.208

[1] The coherent scattering coefficients tabulated by Hubbell [13] are converted to units m^{-1} by using density of 1.04 g cm^{-3} from ICRP 23 [14] for muscle.

4. Conclusion

The differences between experimental and theoretical molecular FF have repercussions upon total coherent scattering cross sections (σ_{mol}). As molecular form factors vary importantly for low x values, coherent cross sections differ significantly for low photon energies. Both molecular form factors and coherent cross section differences are due to interference effects.

References

[1] Leliveld, C.J., Maas, J.G., Bom, V.R. and van Eijk, C.W.E., Monte Carlo modelling of coherent scattering: Influence of interference, **IEEE Transactions on Nuclear Science**, 43, 3315-3321, (1996).

[2] Tartari, A., Taibi, A., Bonifazzi, C. and Baraldi, C., Updating of form factor tabulations for coherent scattering of photons in tissues, **Physics in Medicine and Biology,** 47, 163-175, (2002).

[3] Baró, J., Roteta, M., Fernández-Varea, J.M. and Salvat, F., Analytical cross sections for Monte Carlo simulation of photon transport, **Radiation Physics and Chemistry**, 44, 531-552, (1994).

[4] İçelli, O. and Erzeneoğlu, S., A new method for the determination of molecular scattering differential cross sections in some lanthanide compounds with energy dispersive x-ray fluorescence system, **Nuclear Instruments and Methods in Physics Research Section B: Beam Interactions with materials and Atoms**, 215, 9-15, (2004).

[5] Akça, B. and Erzeneoğlu, S., The Determination of Molecular Scattering Differential Cross Sections for Compounds of Some Essential Elements at 3.38 1/Angstrom Photon-Momentum Transfer, **Canadian Journal of Physics**, 94, 1-4, (2016).

[6] Taibi, A., Royle, G.J. and Speller, R.D., A Monte Carlo simulation study to investigate the potential of diffraction enhanced breast imaging, **IEEE Transactions on Nuclear Science**, 47, 1581-1586, (2000).

[7] Harding, G. and Schreiber, B., Coherent x-ray scattering imaging and its applications in biomedical sciences and industries, **Radiation Physics and Chemistry**, 56, 229-245, (1999).

[8] Leclair, R.J. and Johns, P.C., X-ray forward-scatter imaging: Experimental validation of model, **Medical Physics**, 28, 210-219, (2001).

[9] Morin, L.R.M., Molecular form factors and photon coherent scattering cross sections of water, **Journal of Physical and Chemical Reference Data**, 11, 1091-1098, (1982).

[10] Peplow, D.E. and Verghese, K., Measured molecular coherent scattering form factors of animal tissues, plastics and human breast tissue, **Physics in Medicine and Biology**, 43**,** 2431-2452, (1998).

[11] King, B.W., Landheer, K.A. and Johns, P.C., X-ray coherent scattering form factors of tissues, water and plastics using energy dispersion, **Physics in Medicine and Biology**, 56, 4377-4397, (2011).

[12] Rao, D.V., Takeda, T., Itai, Y., Akatsuka, T., Cesareo, R., Brunetti, A. and Gigante, G.E., X-Ray scattering cross sections for molecules, plastics, tissues, and few biological materials, **Journal of Trace and Microprobe Techniques**, 20, 327-361, (2002).

[13] Hubbell, J.H., Photon cross sections, attenuation coefficients, and energy absorption coefficients from 10 keV to 100 GeV, **NSRDS-NBS**, 29,1-80, (1969).

[14] ICRP (International Commission on Radiological Protection) Report of the Task Group on Reference Man ICRP Report 23, Oxford: Pergamon, (1975).

[15] Kosanetzky, J., Knoerr, B., Harding, G. and Neitzel, U., X-ray diffraction measurements of some plastic materials and body tissues, **Medical Physics**, 14, 526-532, (1987).

[16] Böke, A., Calculation of the total Rayleigh scattering cross sections of photons in the energy range of 30-50 keV for Nb and Mo elements, **Radiation Physics and Chemistry**, 80, 609-613, (2011).

[17] Hubbell, J.H., Veigele, W.J., Briggs, E.A., Brown, R.T., Cromer, D.T. and Howerton, R.J., Atomic form factors, incoherent scattering functions, and photon scattering cross sections, **Journal of Physical and Chemical Reference Data**, 4, 471-538, (1975).

[18] Hubbell, J.H. and Øverbø, I., Relativistic atomic form factors and photon coherent scattering cross sections, **Journal of Physical and Chemical Reference Data**, 8, 69-105, (1979).

[19] Schaupp, D., Schumacher, M., Smend, F., Rullhusen, P. and Hubbell, J.H., Small-angle Rayleigh Scattering of Photons at High Energies: Tabulations of Relativistic HFS Modified Atomic Form Factors, **Journal of Physical and Chemical Reference Data**, 12, 467-512, (1983).

[20] Chantler, C.T., Detailed tabulation of atomic form factors, photoelectric absorption and scattering cross section, and mass attenuation coefficients in the vicinity of absorption edges in the soft X-ray (Z=30-36, Z=60-89, E= 0.1 keV-10 keV), addressing convergence issues of earlier work, **Journal of Physical and Chemical Reference Data**, 29, 597-1056, (2000).

[21] Zhou, B. and Pratt, R.H., Calculation of Anomalous scattering for ions and atoms, **Physica Scripta,** 41, 495-498, (1990).

[22] Bradley, D.A. and Ghose, A.M., Total-atom differential coherent-scattering crosssection measurements on Sn and Pb using moderate-energy γ rays, **Physical Review A,** 33, 191-204, (1986).

[23] Bradley, D.A., Gonçalves, O.D. and Kane, P.P., Measurements of photon–atom elastic scattering cross-sections in the photon energy range 1 keV to 4 MeV, **Radiation Physics and Chemistry,** 56, 125-150, (1999).

[24] Bradley, D.A., Roy, S.C. and Kissel, L., Pratt, R.H., Anomalous scattering effects in elastic photon–atom scattering from biomedically important elements, **Radiation Physics and Chemistry,** 56, 175-195, (1999).

[25] Eichler, J., de Barros, S., Gonçalves, O. and Gaspar, M., Comparison of Compton and Rayleigh scattering at 145 keV, **Physical Review A,** 28, 3656-3658, (1983).

[26] Siddappa, K., Nayak, N.G., Balakrishna, K.M. and Lingappa, N., Experimental studies on atomic form factors at 4.808-$Å^{-1}$ photon momentum transfer, **Physical Review A,** 39, 5106-5110, (1989).

[27] Kissel, L., Pratt, R.H. and Roy, S.C., Rayleigh scattering by neutral atoms, 100 eV–10 MeV, **Physical Review A,** 22, 1970-2004, (1980)**.**

[28] Kissel, L., RTAB: the Rayleigh scattering database, Radiat, **Radiation Physics and Chemistry,** 59, 185-200, (2000).

[29] Nayak, N.G. and Siddappa, K., Experimental atomic form factors of some rare earth and heavy elements by coherent scattering of 145.4 keV gamma rays, **Radiation Physics and Chemistry,** 71, 673-675, (2004).

[30] İçelli, O. and Erzeneoğlu, S., Coherent scattering of 59.5 keV γ-rays by ^{79}Au through angles from 451˚ to 1251˚, **Spectrochimica Acta Part B,** 56, 331-335, (2001).

[31] Kane, P.P., Mahajani, J., Basavaraju, G. and Priyadarsini, A.K., Scattering of 1.1732-and 1.3325 MeV gamma rays through small angles by carbon, aluminum, copper, tin, and lead, **Physical Review A,** 28, 1509-1516, (1983).

[32] Kane, P.P., Elastic scattering of gamma rays and X-rays, **Radiation Physics and Chemistry,** 74, 402-410, (2005).

[33] Roy, S.C. and Kissel, L., Pratt, R.H., Elastic photon scattering at small momentum transfer and validity of form-factor theories, **Physical Review A,** 27, 285-290, (1983).

[34] Roy, S.C., Zhou, B., Kissel, L. and Pratt, R.H., Rayleigh scattering and form factors, **Indian Journal of Physics B**, 67, 481-496 , (1993).

[35] Roy, S.C., Kissel, L. and Pratt, R.H., Elastic scattering of photons, **Radiation Physics and Chemistry,** 56, 3-26, (1999).

[36] Chan, H.P. and Doi, K., Energy and angular dependence of x-ray absorption and its effect on radiographic response in screen-film systems, **Physics in Medicine and Biology**, 28, 565-579, (1983).

[37] Tartari, A., Casnati, E., Bonifazzi, C. and Baraldi, C., Molecular differential cross sections for x-ray coherent scattering in fat and polymethyl methacrylate, **Physics in Medicine and Biology**, 42, 2551-2560, (1997).

[38] Tartari, A., Bonifazzi, C., Fernandez, J.E., Bastiano, M., Casnati, E., Baraldi, C. and Di Domenico, G., Molecular coherent scattering data for tissue in photon transport Monte Carlo codes, **Applied Radiation and Isotopes**, 53, 901-906, (2000).

[39] Tartari, A., Taibi, A., Bonifazzi, C., Gambaccini, M. and Marina, F., Updating of x-ray coherent scattering cross-sections and their effects in microbeam and material analysis applications, **X-Ray Spectrometry**, 34, 421-425, (2005).

[40] Thomson, J.J., **Conduction of electricity through gases**, Cambridge University Press, Cambridge, (1906).

[41] Narten, A.H. and Levy, H.A., **Water: A Comprehensive Treatise**, In: Franks, F. Ed. vol 1, p. 311, Plenum Press, New York, London, (1972).

[42] Tartari, A., Bonifazzi, C. and Casnati, E., Photon scattering data from X-ray diffraction pattern measurements: correction procedure evaluation, **Nuclear Instruments and Methods B**, 142, 203-209, (1998).

[43] King, B.W. and Johns, P.C., An energy-dispersive technique to measure x-ray coherent scattering form factors of amorphous materials, **Physics in Medicine and Biology**, 55, 855-871, (2010).